

1 **Machine learning enables accurate prediction of breast** 2 **cancer five-year survival using somatic genomic variants**

3 Xiaosen Jiang^{1,2}, Laizhi Zhang³, Guangshuo Cao⁴, Jia Li^{5,6}, Yong Bai^{2*}

4

5 1 College of Life Sciences, University of Chinese Academy of Sciences, Beijing 100049, China.

6 2 BGI-Shenzhen, Shenzhen, China.

7 3 School of Basic Medicine, QINHGDAO University.

8 4 State Key Laboratory of Public Big Data, College of Computer Science and Technology,

9 Guizhou University, Guiyang, 550025, China.

10 5 BGI Genomics, BGI-Shenzhen, Shenzhen, 518083, China.

11 6 Hebei Industrial Technology Research Institute of Genomics in Maternal & Child Health,

12 Shijiazhuang BGI Genomics Co., Ltd, Shijiazhuang 050000, Hebei Province, China.

13

14 * Correspondence:

15 Yong Bai

16 baiyong@genomics.cn

17

18 **Abstract**

19 Breast cancer is one of the most common cancers, accounting for about 30% of
20 female cancers and a mortality rate of 15%. The 5-year survival rate is most
21 commonly used to assess cancer progression and guide clinical practice. We used the
22 CatBoost model to systematically construct a five-year mortality risk prediction
23 model based on two independent data sets (BRCA_METABRIC, BRCA_TCGA). The
24 model input data are the somatic genomic variants (copy number variation, SNP locus,
25 cumulative mutation number of genes) and phenotype data of cancer samples. The
26 optimal model combined all the above characteristics, and the AUC reached 0.70 in
27 an independent external data set. At the same time, we also conducted a biological
28 analysis of the characteristics of the model and found some potential biomarkers

29 (TP53, DNAH11, MAP3K1, PHF20L1, etc.). The results of model risk stratification
30 can be used as a guide for the prognosis of breast cancer.

31 **Introduction**

32 Breast cancer has overtaken lung cancer to become the most common malignancy
33 and the first leading lethal cancer among women, accounting for approximately 11.7%
34 of all cancer cases diagnosed (2.3 million) in 2020 around the world[1]. In spite of
35 significant medical improvements in early diagnosis and modern therapy [2], breast
36 cancer still poses increasing burden globally and the overall survival outcomes remain
37 unsatisfactory given the mortality of 1 in 6 female cancers (685,000 deaths)[1],
38 reflecting high biological complexity and genetic heterogeneity of the disease[3-5].
39 Consequently, identification of genetic prognostic indicators plays crucial roles in
40 understanding inter-individual differences in pathogenesis between breast cancer
41 patients, providing better insight into therapeutic decision-making and optimizing
42 personalized precise treatment. Additionally, the prognosis of breast cancer, which has
43 a 5-year survival rate greater than 85%, is better than other cancers[6]. Since the
44 threshold of five years is most commonly used to assess the process of the cancer, we
45 can anticipate the 5-year mortality of breast cancer to guide clinical intervention.

46 One of the earliest survival prognostic models, Nottingham Prognostic
47 Index(NPI)[7], was constructed based on clinical factors using Cox regression[8].
48 Since then, more variables had been considered to improve the accuracy of NPI[9]. In
49 2001, Adjuvant, an internet-based tools was developed and widely applied in
50 prognosis analysis in breast cancer[10]. In 2010, two independent models,

51 OPTIONS[11] based on parametric regression and PREDICT based on Cox
52 proportional hazards, were established. But both Adjuvant and PREDICT showed low
53 accuracy of estimating mortality in different sub-groups, especially for young breast
54 cancer patients[12]. Additionally, these statistically constructed models based on
55 clinical data are limited by the prolonged process of data collecting and poor
56 timeliness. These drawbacks entail the need for prediction using data collected right
57 after diagnosis. With the advent of microarray-based gene expression profiling, some
58 gene-related studies demonstrate the impact of genetic factors on prognostic and
59 survival prediction of breast cancer and lots of predictive signatures have been
60 found[13]: such as MammaPrint[14], Oncotype DX[15], Endopredict[16]. Although
61 these models are applied to sub-groups of breast cancer patients, their signatures
62 cannot sensibly interpret their relationships with breast cancer outcomes, which are
63 called black-box models[17]. Thus models with high accuracy and high
64 interpretability need to be further developed.

65 Machine learning(ML) is a feasible method, since ML can extract features from
66 large genetic datasets and perform risk scoring and classification[18]. Genetic
67 signature copy number alteration(CNA) has a strong correlation with the prognosis
68 and mortality of cancer[19]. However, because the genomic CNA dataset is large and
69 relatively sparse, traditional models based on single or several CNA signatures are not
70 explicable. Furthermore, Somatic mutations can also be used to construct predictive
71 models for risk scoring and survival prediction. Nguyen et al. selected multi-features
72 with Random Forest(RF), largely improving the accuracy of the predictive model[20].

73 Support Vector Machine(SVM), Artificial Neural Network(ANN) and
74 semi-supervised learning methods were employed to construct predictive models for
75 assessing the survivability of breast cancer patients[21]. Compared to the integrated
76 model, the models based on somatic mutations alone have lower accuracies, and
77 integrated models are limited by small samples and may have overfitting problems[22,
78 23]. We found that most of the reported 5-year survival prediction models for breast
79 cancer have considered data preprocessing, feature selection, class imbalance
80 processing, and model validation.[24]. We only find two studies that were further
81 verified externally[25, 26]. Both of the studies used the Molecular Taxonomy of
82 Breast Cancer International Consortium(BRCA_METABRIC) dataset for training and
83 internal validation, and The Cancer Genome Atlas(BRCA_TCGA) dataset was used
84 for further validation. However, after scrutinizing these two studies, we found that
85 their independent dataset, which should be used for external test, was fed into their
86 models for training and internal testing again. External validation is necessary because
87 it can reflect the generalization ability of the predictive model. So far as we know,
88 there is no breast-survival-predictor that undertakes external test using independent
89 cancer datasets.

90 In our study, we developed a CatBoost-based machine learning model that
91 integrates multi-dimensional data including single-nucleotide variants(SNV),
92 cumulative number of gene mutations(CNGM) ,copy number alteration(CNA) and
93 phenotype data. BRCA_METABRIC dataset was employed for training and internal
94 validation and BRCA_TCGA dataset for external testing. The final result of the model

95 has good generalization ability, and the AUC in the external test set is 0.70. In
96 addition, the feature interpretation of the model found that the model has a high
97 learning ability, and some features that have been reported to be highly related to
98 cancer were found in the model. The code required by the model can be viewed in
99 github: https://github.com/jxs1996/Breast_cancer-5-year-survival-prediction

100 **Materials and methods**

101 **Data preparation**

102 We obtained two breast cancer data sets from the public database
103 cBioPortal(BRCA_TCGA(n=1108 samples)[27],
104 https://www.cbioportal.org/study/summary?id=brca_tcga;
105 BRCA_METABRIC(n=2509 samples) [28-30],
106 https://www.cbioportal.org/study/summary?id=brca_metabric). Overall, the median
107 age was 62□years; the 5-year survival rate was 75%. Both data sets contain clinical
108 data, somatic mutations, CNA and gene expression data. In the preliminary data
109 processing(Figure1.A), The SNV, CNGM, and CNA features in the two data sets were
110 separately counted and constructed into the input data required by the model.
111 Predictive features were expressed as follows: (1)SNV: if there is a mutation, it is
112 marked as "1", if it is not marked as "0"; CNGM: each additional SNV, the value
113 increases by 1, and each additional insertion or deletion, the value increases by 10
114 (This is because we assume that insertions and deletions have a greater accumulation
115 of mutations and a greater impact on genes than SNV); CNA: “-2” for homozygous
116 deletion, “-1” for hemizygous deletion, “0” for neutral / no change, “1” for gain, “2”

117 for high level amplification. The missing values of all features are filled with “0”.

118 Gene expression data is not included in the feature representation. There are two main

119 reasons. 1) The data obtained from the two datasets are standardized with Z-score,

120 which means they are not in the same spatial dimension. Training results in one data

121 cannot be applied in another dataset; 2) If genomic data alone yields better prediction

122 results. This can significantly reduce the cost of the application. Nevertheless, gene

123 expression data will be used in subsequent analysis to observe the performance of the

124 model features at the transcriptome level. In order to ensure the consistency of

125 features, the intersection of SNV, CNGM and CNA is obtained in two independent

126 datasets. Next, we labeled samples as survival($OS_Months > 60$) or

127 death($OS_MONTHS < 60$ and $OS_Status = deceased$). Some sample data were

128 discarded($OS_MONTHS < 60$ and $OS_STATUS = LIVING$).

129 We retained a total of CNA - 18533, SNV - 215, CNGM - 170 in both datasets.

130 BRCA_METABRIC dataset retained 1904 individuals (survival - 1432, death - 412,

131 discarded - 60), BRCA_TCGA dataset retains 513 individuals (survival-148, death-46,

132 discard-319). In addition, we screened the clinical data shared by the two

133 datasets (because we hope to establish an early risk prediction model, the data of

134 intervention treatment will not be considered), and finally obtained age, gender,

135 number of positive lymph nodes and menopausal state. Most patients are female (there

136 are only three males in the BRCA_TCGA dataset), so the sample is no longer grouped

137 by gender. The statistical results of other phenotypes are shown in Supplementary

138 Figure S1. The average age of all breast cancer patients is 60.65 years, and the

139 average lymph node is 2.02. 443 are not yet menopausal, and 1548 are in menopause.
140 If there is no measurement data in the phenotype, it will be represented by -9 and will
141 not participate in the mean calculation.

142 **Machine learning analysis process development**

143 As shown in Figure 1.B, Catboost, a high-performance open source library for
144 gradient boosting on decision trees, was developed to predict the five-year mortality
145 risk of patients. The analysis process is systematically constructed using the machine
146 learning framework scikit-learn(<https://scikit-learn.org/stable/>, version=0.24.2). The
147 BRCA_METABRIC data(1844 samples: survival-1432, death-412) set was split into
148 training set(80%) and testing set(20%) by random stratified sampling. The
149 independent external data set BRCA_TCGA (194 samples: survival-148, death-46)
150 will be used for model evaluation. For the three features(SNV, CNA, CNGM),
151 separate models are established to evaluate their effects on prediction. After that, we
152 extract the model features constructed by SNV, CNA, and CNGM and merge them to
153 construct a new multi-dimensional feature set for training and evaluation. Finally,
154 phenotypic characteristics (age, number of positive lymph nodes, menopausal status)
155 are also integrated to further improve the accuracy of the model.

156 **Single-dimensional feature model construction**

157 Separate models were constructed for CNV, SNV, and CNGM characteristics to
158 explore their impact on the five-year mortality risk prediction. As shown in Figure 1.B,
159 For CNA (18533 features), the training set is first standardized (StandardScaler
160 method), the average value and standard deviation are retained and then applied to the

161 corresponding features in the test phase, and feature selection is performed on the
162 processed data (described in Feature selection part). Next, use the CatBoost model to
163 select the hyperparameters of the model (described in Hyperparameter selection part).
164 After fixing the hyperparameters, perform model training. Five-fold cross-validation
165 is used to evaluate the stability of the model, and finally tested on the test set and
166 independent external data set. The processing of SNV and CNGM is similar to CNA,
167 but due to the small number of SNV features (215) and onehot-encoded, data
168 standardization and feature selection are not performed; CNGM uses log first and then
169 logMinMaxScaler method during standardization. Since there are only 170 features,
170 feature selection is also omitted.

171 **Multi-dimensional feature model construction**

172 Combine the feature selection results of the single-dimensional feature model and
173 perform hyperparameter selection (described in Hyperparameter selection part). After
174 the hyperparameter results are fixed, perform training and evaluation. In addition, we
175 combined the phenotypic data (age, gender, number of positive lymph nodes, and
176 menopausal status) with the feature selection results of the single-dimensional feature
177 model to observe whether the phenotypic data can improve the performance of the
178 model.

179 **Feature selection**

180 For CNA(18533 features), irrelevant features may decrease the performance of
181 the model. We propose a hybrid feature selection method to subtract features. In this
182 method, mutual information (MI) technology[31], recursive feature elimination (RFE)

183 algorithm[32] and Boruta algorithm[33] are used to obtain the relevant subset of the
184 raw features. MI calculates feature weights based on the relationship between features
185 of mutual information; RFE selects features by recursively considering smaller and
186 smaller feature sets, and this method can obtain all feature rankings. The Boruta
187 algorithm is a packaging method that selects a subset of features based on a random
188 forest machine learning algorithm, which can be used to measure the importance of
189 features. Respectively use the above methods to obtain the feature ranking and retain
190 the top 3% features (extract the most effective features and maintain a balance with
191 the SNV and CNGM feature numbers). The features selected by any two methods will
192 be retained eventually.

193 **Hyperparameter selection**

194 Due to the imbalance between death and survival samples (~1:3), when 80% of
195 the training set is used for hyperparameter training, a small number of samples are
196 randomly sampled to make the ratio of positive and negative samples reach 1:1. We
197 implemented a basic grid search algorithm with 5-fold cross-validation to optimize
198 the Catboost model parameters while maximizing the weighted F1 score.

199 **Model comparison**

200 After the model training is completed, we will use the five-fold cross-validation
201 data set, test set and independent external data set to evaluate the model. The specific
202 evaluation indicators are as follows:

203 *TP*: True Positive. In the samples judged to be positive, the number of correct
204 judgments.

205 *FP*: False Positive. In the samples judged as positive, the number of judgment
206 errors.

207 *TN*: True Negative. Among the samples judged as negative, the correct number is
208 judged.

209 *FN*: False Negative. In the samples judged as negative, the number of judgment
210 errors.

$$211 \quad Accuracy = \frac{TP + TN}{TP + TN + FN + FP}$$

212 (1)

$$213 \quad Precision = \frac{TP}{TP + FP} \quad (2)$$

$$214 \quad Recall = \frac{TP}{TP + FN}$$

215 (3)

216 *AUC*: The area under the receiver operating characteristic(ROC) curve, is
217 currently considered to be the standard method to assess the accuracy of predictive
218 distribution models[34]. with $AUC = 1$ represents perfect performance and 0.5 means
219 random guess.

220 *F1-score*: The harmonic mean of the precision(2) and recall(3). The highest
221 possible value of an F-score is 1.0, indicating perfect precision and recall, and the
222 lowest possible value is 0, if either the precision or the recall is zero.

223 **Feature analysis**

224 We will select the model with the best comprehensive score and use the
225 SHAP(Shapley Additive exPlanations) tool to analyze the characteristics of the final
226 model[35]. SHAP is a unified method to explain machine learning predictions based

227 on the optimal Shapley value of game theory. SHAP computed the contribution of
228 each feature to the prediction, which was quantified using Shapley values from
229 coalitional game theory. The Shapley value was represented as an additive feature
230 attribution method, providing the average of the marginal contributions across all
231 permutations of features and distribution of model prediction among features. As an
232 alternative to permutation feature importance, SHAP feature importance was based on
233 magnitude of feature attributions. The absolute Shapley values per feature across the
234 data was further averaged as the global importance was needed. We ranked the
235 features importance in descending order and picked the top 30 most important
236 features. The SHAP value can be plotted for each sample corresponding to the first 30
237 features. We used the Python library to implement the SHAP algorithm
238 (<https://github.com/slundberg/shap>).

239 For features, the enrichment analysis in CLINVAR, KEGG, GO, and Reactome
240 will also be performed using ClueGO[36]. In addition, the genes corresponding to the
241 optimal model features were extracted, and the Kruskal-Wallis test was used in the
242 BRCA_METABRIC gene expression data set (Bonferroni correction of the results,
243 adjusted P value ≤ 0.05) to calculate the difference between survival and death
244 groups. For genes with significant differences, use the limma tool[37] to calculate the
245 expression fold difference.

246 **Risk stratification analysis**

247 The original output result of the model is a probability value (between 0 and 1).
248 Based on the optimal model result, We will divide all samples into high, medium and

249 low risk groups (BRCA_METABRIC, BRCA_TCGA), and draw Kaplan-Meier (K-M)
250 curve.

251 **Result**

252 **Comparison of performance of different machine learning models**

253 The optimization process of the five models (CNA, SNV, CNGM,
254 SNV+CNGM+CNA(combined variants) , combined variants+phenotype)was shown
255 in Supplementary Figure S2. The number of features and AUC values corresponding
256 to the optimal model were: SNV(AUC:0.56; features: 93), CNGM(AUC:0.63;
257 features: 4), CNA(AUC:0.64; features: 75), combined variants (AUC:0.72; features:
258 353), combined variants + phenotype (AUC:0.81; features: 172).

259 We have drawn the Precision-Recall and ROC curves for the above optimal
260 models using the 5-fold cross-validation method in the BRCA_METABRIC, internal
261 test set and external test set (Figure 2). Taking the test result of the external data set
262 BRCA_TCGA as the final evaluation index, the indexes of each model are as follows:
263 SNV(AUC:0.53, APS:0.25); CNGM(AUC:0.54, APS:0.26); CNA(AUC:0.62,
264 APS:0.42); combined variants (AUC:0.61, APS:0.35); combined
265 variants+phenotype(AUC:0.70, APS:0.43); More model evaluation indicators can be
266 viewed in Table 1. The best comprehensive score was the combined
267 variants+phenotype model, which performed best in both the internal test set
268 (AUC:0.81, APS:0.55) and the independent external data set (AUC=0.70,
269 APS:0.43)(Table 1).

270 **Optimal model feature ranking**

271 The combined variants + phenotype model comprised a total of 172 features,
272 including 121 CNA, 45 CNGM, 4 SNV, and 2 phenotypes (age, number of positive
273 lymph nodes). We used shap to analyze the importance of the predictive characteristics
274 of the model. As shown in Figure 3, among the 172 features of the model, we
275 extracted the top 30 most important features. The phenotypic characteristics age and
276 number of positive lymph nodes ranked first and second, and showed positive
277 correlation with death within five years. The remaining 28 features included 18 CNA
278 (ZNF720, TBC1D13, SCAF4, CDRT15, TMED6, OR4M2, C17orf102, TAS2R10,
279 PHF20L1, RNF187, STIM2, CCDC136, TTI2, MTBP, FAM24B, TMEM26, OR4F15,
280 PDCL2), 9 CNGM (TP53, DNAH11, DNAH2, PIK3CA, MAP3K1, GATA3, CDH1,
281 PDE4DIP, 80273), 1 SNV(chr3:178936091:G:A). Some characteristics also showed
282 positive correlation with mortality within five years, such as CNGM-TP53,
283 CNGM-DNAH2, CNGM-PIK3CA, CNA-SCAF4, CNGM-CDH1, etc. There were
284 also some opposite manifestations, such as CNA-ZNF720, CNGM-DNAH11,
285 CNA-TMED6, CNGM-MAP3K1, SNP-3-178936091-G-A, etc.

286 **Enrichment analysis of optimal model features**

287 We used ClueGO to perform enrichment analysis on the genes corresponding to
288 172 features. The selected data sets included CLINVAR, KEGG, GO, and Reactome
289 pathways. The enrichment results were corrected by bonferoni multiple test. After
290 correction, the pathways with adjusted P value less than 0.05 were selected(Figure
291 4.A). A total of 33 records were obtained. In CLINVAR and KEGG, the features were
292 enriched in pan-cancer or breast cancer-related pathways (C0006142, C1458155,

293 KEGG:05212, KEGG:05222, KEGG:05224). In GO biological process pathways,
294 these genes were over-represented in some pathways related to cell cycle and cell
295 proliferation (GO:0048103, GO:1904030, GO:0000079, GO:0061982, etc.). Two
296 REACTOME pathways reached statistical significance, both of which are related to
297 the NOTCH signaling pathway (R-HSA: 350054, R-HSA: 1980143)

298 **Difference analysis of features at the transcriptoional level**

299 In the optimal model, we extracted the genes corresponding to 170 features
300 (excluding two phenotypic features). In BRCA_METABRIC, a total of 17 genes were
301 differentially expressed between the living and dead breast cancer patient groups
302 (adjusted P value < 0.05 for all cases, Kruskal-Wallis test), such as TP53, DNAH11,
303 MAP3K1, PHF20L1, etc. (Figure 4.B). TP53 (No. 3), DNAH11 (No. 5), MAP3K1
304 (No. 12), PHF20L1 (No. 20) ranked in the top 30 of the model feature weights. The
305 limma results showed that none of these genes had a significant fold change in
306 expression, between the living and dead breast cancer patient groups.

307 **Results of risk stratification**

308 According to the model prediction results of all samples, we assigned samples
309 with probability values less than 0.1(TPR>0.93) to the low-risk group (1473 samples),
310 samples with probability values greater than 0.9(TNR>0.99) to high-risk group (363
311 samples), and others to medium-risk group (202 samples). The stratification results
312 are shown in Figure 5.A. The Kaplan-Meier survival curves corresponding to the
313 three sets of results are shown in Figure 5.B. The results showed that the three groups
314 of patients had significantly different survival outcomes. This has clinical implications.

315 For high-risk patients, more clinical intervention and active treatment may be
316 required.

317 **Discussion**

318 **Model evaluation**

319 The CatBoost algorithm model is used. Different models performed similarly in
320 the training set and the test set without serious overfitting and strong generalization
321 ability. The best model result is the combined variants+phenotype (AUC: 0.70). For
322 a single feature such as SNV, CNGM has a lower AUC In an independent external
323 data set (SNV: AUC=0.53, CNGM: AUC=0.54). CNA, as a single-dimensional
324 feature, is similar to the combined variants model's result in external data
325 set(AUC=0.62), and compared to CNGM and SNV, CNA has better generalization
326 capabilities. But this is also related to the small number of CNA and SNV features,
327 and more comprehensive data needs to be collected for further verification. In
328 addition, the addition of phenotype, especially age and the number of lymph nodes,
329 has a very large impact on death, as can be seen from the feature weights of the
330 optimal model (Figure 3).

331 In general, we comprehensively assessed the impact of different characteristics on
332 the five-year mortality risk. In the process of model evaluation, we found that a single
333 feature has poorer performance than the feature fusion model. CNA accounts for a
334 relatively large number of model features due to the large number of original features,
335 but there are still more CNGM features in the top 30 features. The contribution of
336 SNV features in risk prediction is low. The addition of phenotypic information such as

337 age and number of lymph nodes can increase the accuracy of the model.

338 **Discovery of biomarkers associated with five-year mortality risk**

339 In the optimal combined variants+phenotype model, in addition to phenotypic
340 features, some genomics features that have a greater contribution to the model have
341 also been found. And these features still have significant differences between the
342 survival and death groups at the transcriptome level, although there is no large fold
343 difference. For example, TP53, DNAH11, MAP3K1, PHF20L1. As a very complex
344 biomarker, TP53 acts as a tumor suppressor in many tumor types; induces growth
345 arrest or apoptosis depending on the physiological circumstances and cell type which
346 has been widely reported. Its mutations are widely present in various cancers[38-41].
347 IARC TP53 Database (<https://p53.iarc.fr/>) records all the resources of TP53
348 mutations[41]. They pointed out that there are 28 mutations that lead to a poor
349 prognosis (<https://p53.iarc.fr/SomaticPrognosisStats.aspx>). In our model, the TP53
350 feature comes from the CNGM feature dimension. The model results indicate that the
351 greater the cumulative number of TP53 mutations, the greater the probability of death
352 within five years (Figure. 3). The DNAH11 gene mutation rs2285947 is considered a
353 potential risk factor for ovarian cancer and breast cancer[42], and there is no clear
354 report related to prognosis. MAP3K1 is a component of a protein kinase signal
355 transduction cascade, which has dual regulatory effects on cell survival and apoptosis,
356 and its regulatory mechanism is not yet clear[43, 44]. These characteristics have been
357 reported to be related to cancer, and our study further verified their relationship with
358 the five-year mortality risk.

359 Through feature selection and multi-dimensional feature fusion, the optimal model
360 features are concentrated on pathways related to cancer, cell division, and
361 proliferation without adding additional prior information. This reflects that the design
362 of the model is relatively reliable, and the model can eliminate features that are not
363 related to the training target from a large amount of input data. The genes
364 corresponding to the features retained by the model are potential biomarkers for
365 prognostic analysis and drug development.

366 **Conclusion**

367 In general, in this article, based on the CatBoost algorithm, we use independent
368 data sets of BRCA_METABRIC and BRCA_TCGA to conduct systematic model
369 training on features of different dimensions. The effects of different dimensional
370 features at the genome level on the prediction results of the model are compared. Our
371 best model combines all the features, and the AUC in the external independent
372 BRCA_TCGA is 0.70. In addition, the risk stratification results of all samples showed
373 significant differences between different populations. For high-risk groups classified
374 by the model, active clinical treatment is very necessary. This is the first five-year
375 breast cancer death analysis based on genomic data and using external independent
376 data for evaluation. And compared with other studies, the model based on somatic
377 genomic variants data and phenotypic data (age, number of lymph nodes) is more
378 prospective, and the patient's condition can be evaluated before clinical intervention,
379 providing guidance for follow-up treatment

380 Nevertheless, the research still has limitations. When selecting the features that

381 the two data sets contain in common, the SNP and CNGM features only get very little
382 intersection, which may lead to the underestimation of the role of SNP and CNGM.
383 Deep learning algorithms have not been used and compared. We will continue to
384 conduct in-depth research, collect more comprehensive data, design and develop new
385 algorithms based on existing experience, and further compare the performance
386 differences between machine learning and deep learning. In addition, we will also try
387 to collect other cancer data, conduct migration learning, and develop a five-year
388 mortality risk model for pan-cancer.

389 **Acknowledgments**

390 Thanks to all researchers and subjects who volunteered to participate in this project.

391 **Reference**

- 392 1. Sung, H., et al., *Global cancer statistics 2020: GLOBOCAN estimates of incidence and*
393 *mortality worldwide for 36 cancers in 185 countries*. CA: a cancer journal for clinicians, 2021.
394 **71**(3): p. 209-249.
- 395 2. Loibl, S., et al., *Breast cancer*. Lancet, 2021.
- 396 3. Garcia-Closas, M., et al., *Heterogeneity of breast cancer associations with five susceptibility*
397 *loci by clinical and pathological characteristics*. PLoS genetics, 2008. **4**(4): p. e1000054.
- 398 4. Lüönd, F., S. Tiede, and G. Christofori, *Breast cancer as an example of tumour heterogeneity*
399 *and tumour cell plasticity during malignant progression*. British Journal of Cancer, 2021.
400 **125**(2): p. 164-175.
- 401 5. McClellan, J. and M.-C. King, *Genetic heterogeneity in human disease*. Cell, 2010. **141**(2): p.
402 210-217.
- 403 6. Allemani, C., et al., *Global surveillance of trends in cancer survival 2000-14 (CONCORD-3):*
404 *analysis of individual records for 37 513 025 patients diagnosed with one of 18 cancers from*
405 *322 population-based registries in 71 countries*. Lancet, 2018. **391**(10125): p. 1023-1075.
- 406 7. Haybittle, J.L., et al., *A prognostic index in primary breast cancer*. British Journal of Cancer,
407 1982. **45**(3): p. 361-366.
- 408 8. Cox, D.R., *Regression Models and Life-Tables*. Journal of the Royal Statistical Society. Series
409 B (Methodological), 1972. **34**(2): p. 187-220.
- 410 9. Kattan, M.W., et al., *A tool for predicting breast carcinoma mortality in women who do not*
411 *receive adjuvant therapy*. Cancer, 2004. **101**(11): p. 2509-15.
- 412 10. Ravdin, P.M., et al., *Computer program to assist in making decisions about adjuvant therapy*
413 *for women with early breast cancer*. J Clin Oncol, 2001. **19**(4): p. 980-91.
- 414 11. Campbell, H.E., et al., *Estimation and external validation of a new prognostic model for*

- 415 *predicting recurrence-free survival for early breast cancer patients in the UK*. Br J Cancer,
416 2010. **103**(6): p. 776-86.
- 417 12. Engelhardt, E.G., et al., *Accuracy of the online prognostication tools PREDICT and Adjuvant!*
418 *for early-stage breast cancer patients younger than 50 years*. Eur J Cancer, 2017. **78**: p.
419 37-44.
- 420 13. Reis-Filho, J.S. and L. Pusztai, *Gene expression profiling in breast cancer: classification,*
421 *prognostication, and prediction*. Lancet, 2011. **378**(9805): p. 1812-23.
- 422 14. van 't Veer, L.J., et al., *Gene expression profiling predicts clinical outcome of breast cancer*.
423 Nature, 2002. **415**(6871): p. 530-6.
- 424 15. Paik, S., et al., *A multigene assay to predict recurrence of tamoxifen-treated, node-negative*
425 *breast cancer*. N Engl J Med, 2004. **351**(27): p. 2817-26.
- 426 16. Filipits, M., et al., *A new molecular predictor of distant recurrence in ER-positive,*
427 *HER2-negative breast cancer adds independent information to conventional clinical risk*
428 *factors*. Clin Cancer Res, 2011. **17**(18): p. 6012-20.
- 429 17. Manjang, K., et al., *Prognostic gene expression signatures of breast cancer are lacking a*
430 *sensible biological meaning*. Sci Rep, 2021. **11**(1): p. 156.
- 431 18. Kourou, K., et al., *Machine learning applications in cancer prognosis and prediction*. Comput
432 Struct Biotechnol J, 2015. **13**: p. 8-17.
- 433 19. Hieronymus, H., et al., *Tumor copy number alteration burden is a pan-cancer prognostic*
434 *factor associated with recurrence and death*. Elife, 2018. **7**.
- 435 20. Nguyen, C., Y. Wang, and H.N. Nguyen, *Random forest classifier combined with feature*
436 *selection for breast cancer diagnosis and prognostic*. Journal of Biomedical Science and
437 Engineering, 2013. **Vol.06No.05**: p. 10.
- 438 21. Park, K., et al., *Robust predictive model for evaluating breast cancer survivability*.
439 Engineering Applications of Artificial Intelligence, 2013. **26**(9): p. 2194-2205.
- 440 22. Zhang, Y., et al., *Toward the precision breast cancer survival prediction utilizing combined*
441 *whole genome-wide expression and somatic mutation analysis*. BMC Med Genomics, 2018.
442 **11**(Suppl 5): p. 104.
- 443 23. He, Z., et al., *Integrating Somatic Mutations for Breast Cancer Survival Prediction Using*
444 *Machine Learning Methods*. Front Genet, 2020. **11**: p. 632901.
- 445 24. Li, J., et al., *Predicting breast cancer 5-year survival using machine learning: A systematic*
446 *review*. PLoS One, 2021. **16**(4): p. e0250370.
- 447 25. Sun, D., M. Wang, and A. Li, *A multimodal deep neural network for human breast cancer*
448 *prognosis prediction by integrating multi-dimensional data*. IEEE/ACM Trans Comput Biol
449 Bioinform, 2018.
- 450 26. Arya, N. and S. Saha, *Multi-modal advanced deep learning architectures for breast cancer*
451 *survival prediction*. Knowledge-Based Systems, 2021. **221**: p. 106965.
- 452 27. Tomczak, K., P. Czerwińska, and M. Wiznerowicz, *The Cancer Genome Atlas (TCGA): an*
453 *immeasurable source of knowledge*. Contemporary oncology, 2015. **19**(1A): p. A68.
- 454 28. Curtis, C., et al., *The genomic and transcriptomic architecture of 2,000 breast tumours reveals*
455 *novel subgroups*. Nature, 2012. **486**(7403): p. 346-352.
- 456 29. Pereira, B., et al., *The somatic mutation profiles of 2,433 breast cancers refine their genomic*
457 *and transcriptomic landscapes*. Nature communications, 2016. **7**(1): p. 1-16.
- 458 30. Rueda, O.M., et al., *Dynamics of breast-cancer relapse reveal late-recurring ER-positive*

- 459 *genomic subgroups*. *Nature*, 2019. **567**(7748): p. 399-404.
- 460 31. Kraskov, A., H. Stögbauer, and P. Grassberger, *Estimating mutual information*. *Physical*
461 *review E*, 2004. **69**(6): p. 066138.
- 462 32. Li, F. and Y. Yang. *Analysis of recursive feature elimination methods*. in *Proceedings of the*
463 *28th annual international ACM SIGIR conference on Research and development in*
464 *information retrieval*. 2005.
- 465 33. Kursa, M.B. and W.R. Rudnicki, *Feature selection with the Boruta package*. *J Stat Softw*,
466 2010. **36**(11): p. 1-13.
- 467 34. Lobo, J.M., A. Jimenez-Valverde, and R. Real, *AUC: a misleading measure of the*
468 *performance of predictive distribution models*. *Global Ecology and Biogeography*, 2008. **17**(2):
469 p. 145-151.
- 470 35. Lundberg, S.M. and S.-I. Lee. *A unified approach to interpreting model predictions*. in
471 *Proceedings of the 31st international conference on neural information processing systems*.
472 2017.
- 473 36. Bindea, G., et al., *ClueGO: a Cytoscape plug-in to decipher functionally grouped gene*
474 *ontology and pathway annotation networks*. *Bioinformatics*, 2009. **25**(8): p. 1091-3.
- 475 37. Smyth, G.K., *Limma: linear models for microarray data*, in *Bioinformatics and computational*
476 *biology solutions using R and Bioconductor*. 2005, Springer. p. 397-420.
- 477 38. Bertheau, P., et al., *TP53 status and response to chemotherapy in breast cancer*. *Pathobiology*,
478 2008. **75**(2): p. 132-139.
- 479 39. Børresen Dale, A.L., *TP53 and breast cancer*. *Human mutation*, 2003. **21**(3): p. 292-300.
- 480 40. Petitjean, A., et al., *TP53 mutations in human cancers: functional selection and impact on*
481 *cancer prognosis and outcomes*. *Oncogene*, 2007. **26**(15): p. 2157-2165.
- 482 41. Petitjean, A., et al., *Impact of mutant p53 functional properties on TP53 mutation patterns and*
483 *tumor phenotype: lessons from recent developments in the IARC TP53 database*. *Human*
484 *mutation*, 2007. **28**(6): p. 622-629.
- 485 42. Verma, S., et al., *Genetic variants of DNAH 11 and LRFN 2 genes and their association with*
486 *ovarian and breast cancer*. *International Journal of Gynecology & Obstetrics*, 2020. **148**(1): p.
487 118-122.
- 488 43. Pham, T.T., S.P. Angus, and G.L. Johnson, *MAP3K1: genomic alterations in cancer and*
489 *function in promoting cell survival or apoptosis*. *Genes & cancer*, 2013. **4**(11-12): p. 419-426.
- 490 44. Xue, Z., et al., *MAP3K1 and MAP2K4 mutations are associated with sensitivity to MEK*
491 *inhibitors in multiple cancer models*. *Cell research*, 2018. **28**(7): p. 719-729.

492

493

494 **Figure**

495 **Figure 1. Data quality control and five-year survival prediction model building process. A)**
496 BRCA_TCGA and BRCA_METABRIC data acquisition and quality control process; **B)** In the
497 process of building a polygenic risk assessment model, different processing methods are adopted
498 for different dimension characteristics.

499 **Figure 2. Precision-Recall and ROC curves of optimal models constructed with features of**
500 **different dimensions.** The first row is the ROC curve and the second row is the Precision-Recall
501 curve. From left to right are the results in the cross-validation set(mean), training set and test set,
502 respectively.

503 **Figure 3. Optimal model feature weight analysis.** The scatter points represent the SHAP value
504 of each feature for each sample. Features are sorted according to the sum of the magnitudes of the
505 SHAP values of all samples. The first 30 features are shown, and the colors represent the feature
506 values (red high, blue low). For example, as age ("AGE_AT_DIAGNOSIS") increases, the risk of
507 death within five years of the sample will increase.

508 **Figure 4. A)** Optimal Model Pathway Enrichment Analysis; **B)** Transcriptome-level differential
509 analysis of optimal model features.

510 **Figure 5. A)** Risk stratification for all samples based on model scoring; **B)** Plot Kaplan-Meier
511 survival curves for three groups of stratified outcomes (high, intermediate, and low risk).

512 **Supplementary Figure**

513 **Supplementary Figure S1.** Statistical results of sample distribution regarding gender, number of
514 lymph nodes, menopause (-9 - unknown, 0 - not menopause, 1 - menopause).

515 **Supplementary Figure S2.** The optimization process of the five models (CNA, SNV, CNMG,
516 SNV+CNMG+CNA(combined variants) , combined variants+phenotype).

517

518 **Table**

Model	Internal test data						External test data					
	AUC	F1	Accuracy	precision	recall	APS	AUC	F1	Accuracy	precision	recall	APS
SNV	0.56	0.21	0.72	0.29	0.17	0.25	0.53	0.22	0.70	0.29	0.17	0.25
CNGM	0.63	0.37	0.66	0.32	0.45	0.28	0.54	0.36	0.62	0.30	0.46	0.26
CNA	0.64	0.34	0.74	0.39	0.30	0.34	0.62	0.38	0.77	0.52	0.30	0.42
SNV+CNGM+CNA	0.72	0.32	0.76	0.42	0.26	0.38	0.61	0.25	0.73	0.36	0.20	0.35
SNV+CNGM+CNA +Phenotype	0.81	0.52	0.80	0.55	0.49	0.55	0.70	0.46	0.77	0.51	0.41	0.43

519 **Table 1.** The model predicts the performance indicators of breast cancer deaths within five years

520 in the internal and external test data sets.

521

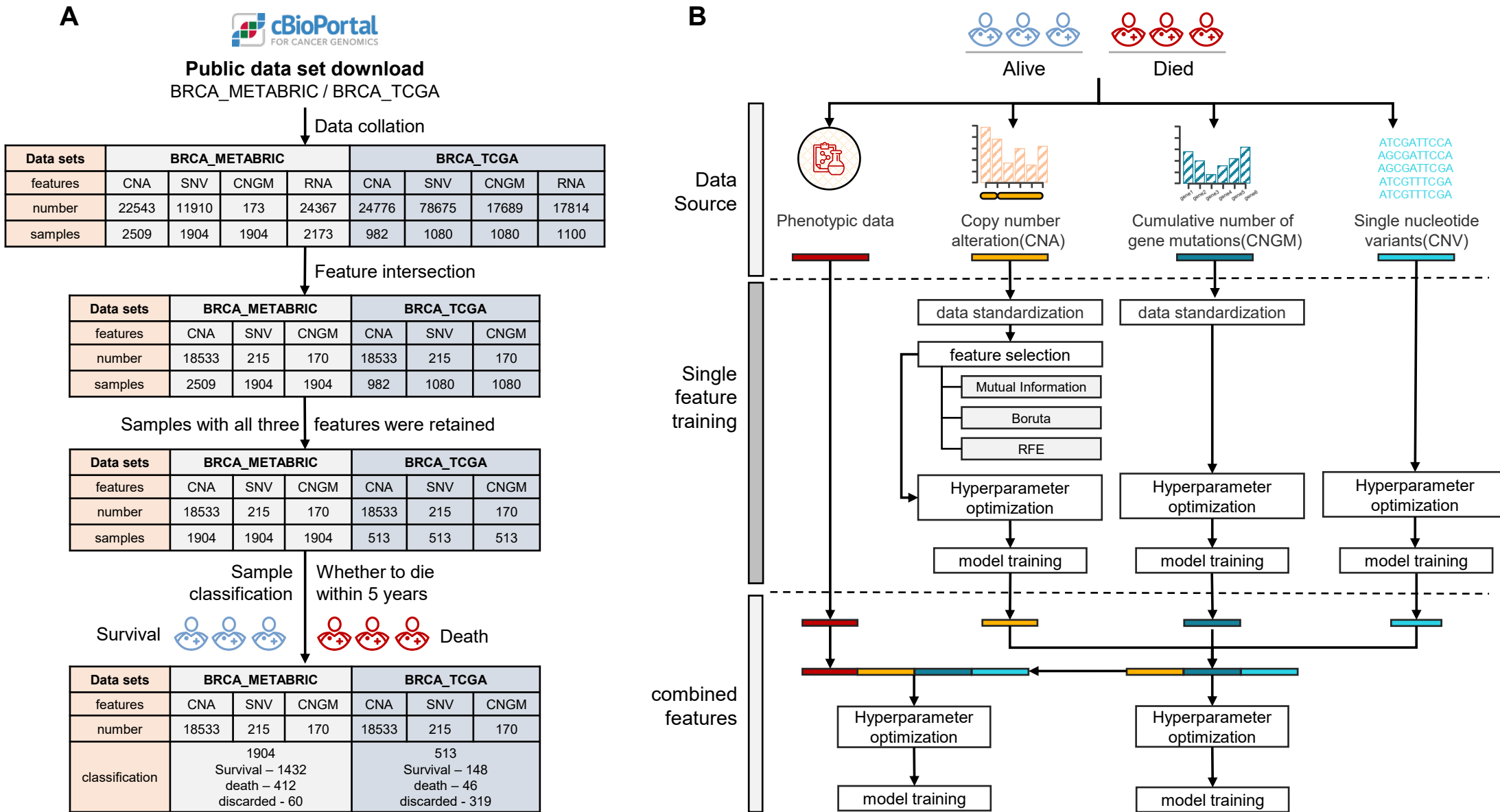


Figure 1. Data quality control and five-year survival prediction model building process. A) BRCA_TCGA and BRCA_METABRIC data acquisition and quality control process; B) In the process of building a polygenic risk assessment model, different processing methods are adopted for different dimension characteristics.

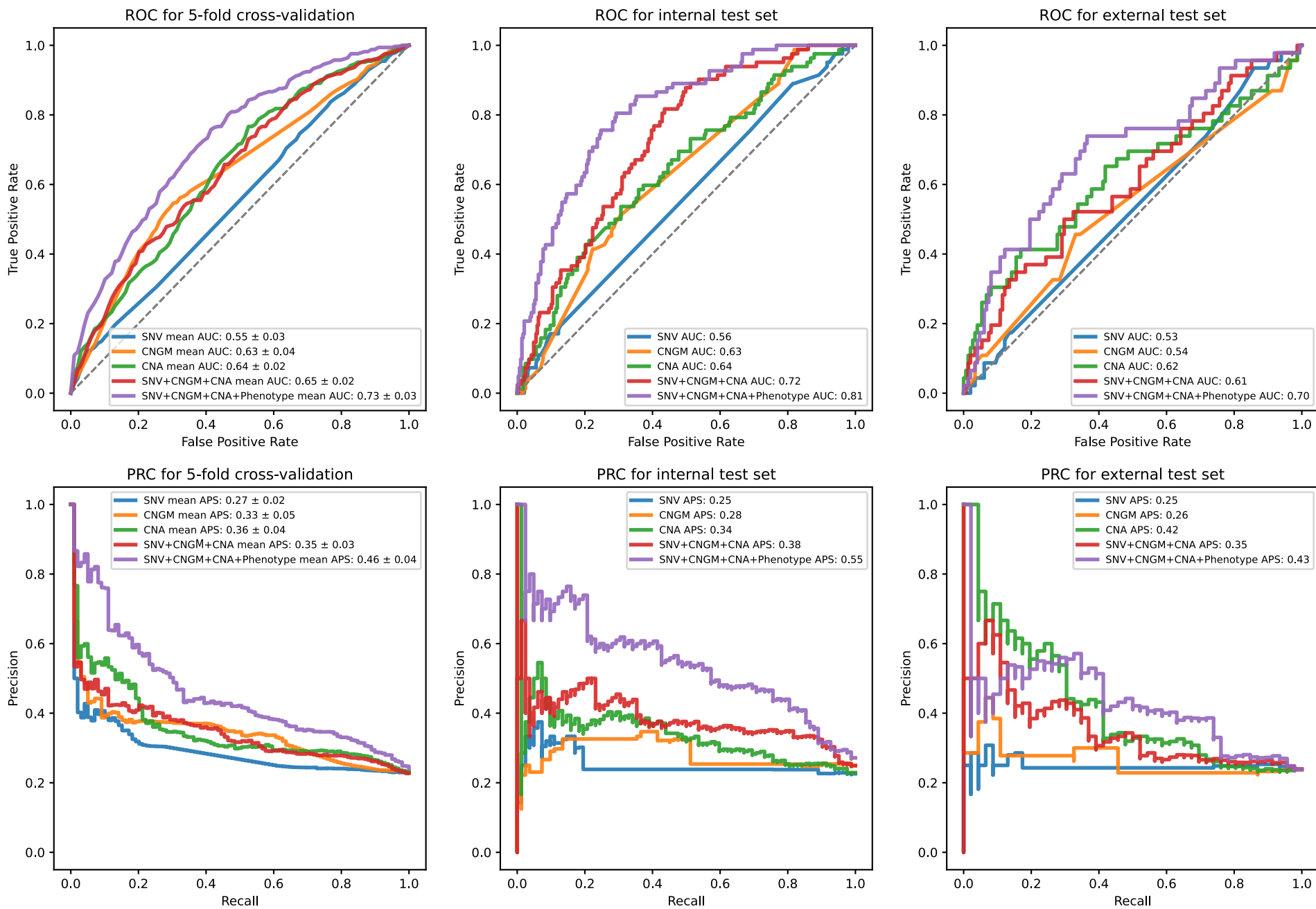


Figure 2. Precision-Recall and ROC curves of optimal models constructed with features of different dimensions. The first row is the ROC curve and the second row is the Precision-Recall curve. From left to right are the results in the cross-validation set(mean), training set and test set, respectively.

LYMPH_NODES_EXAMINED_POSITIVE

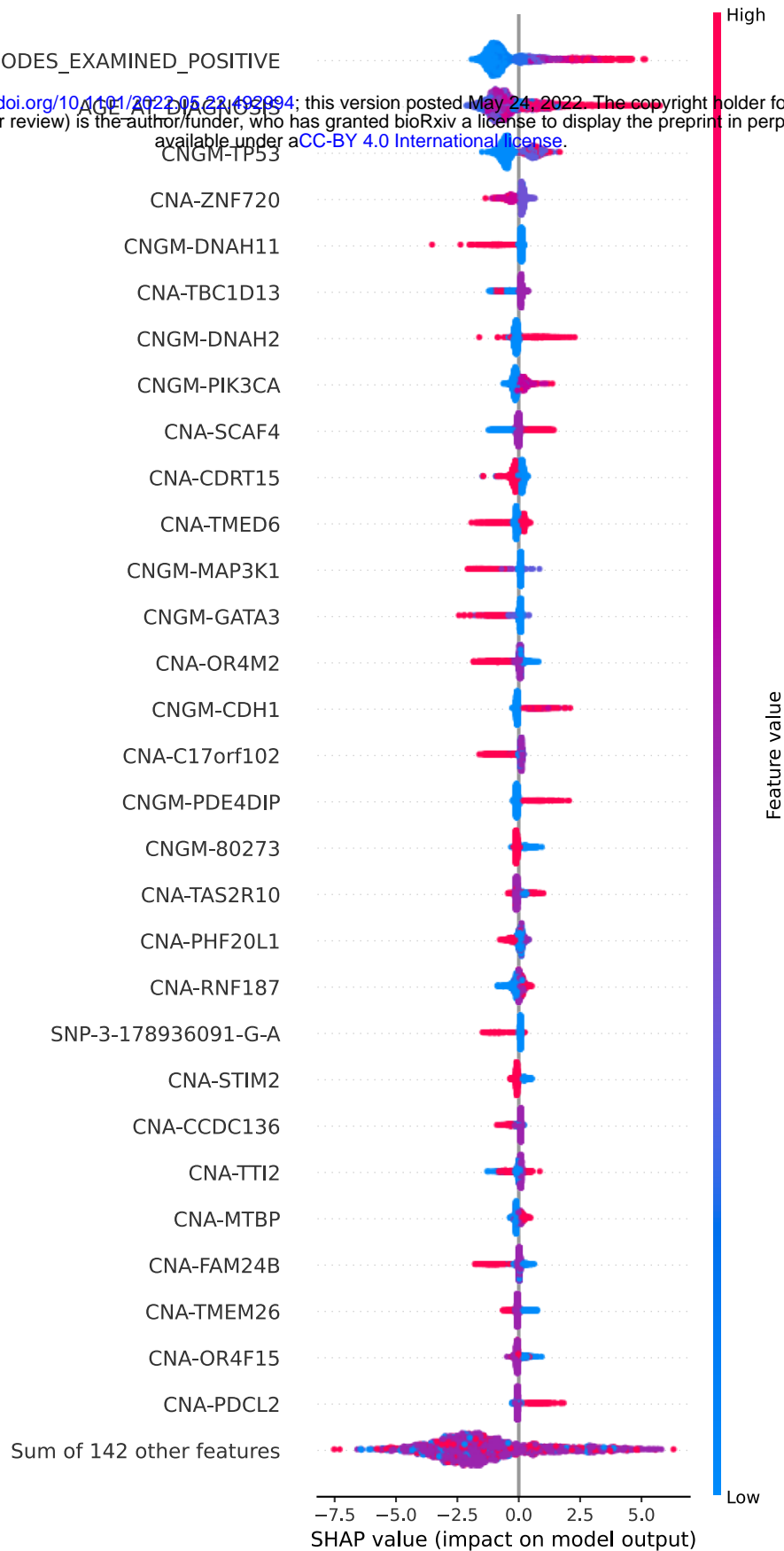
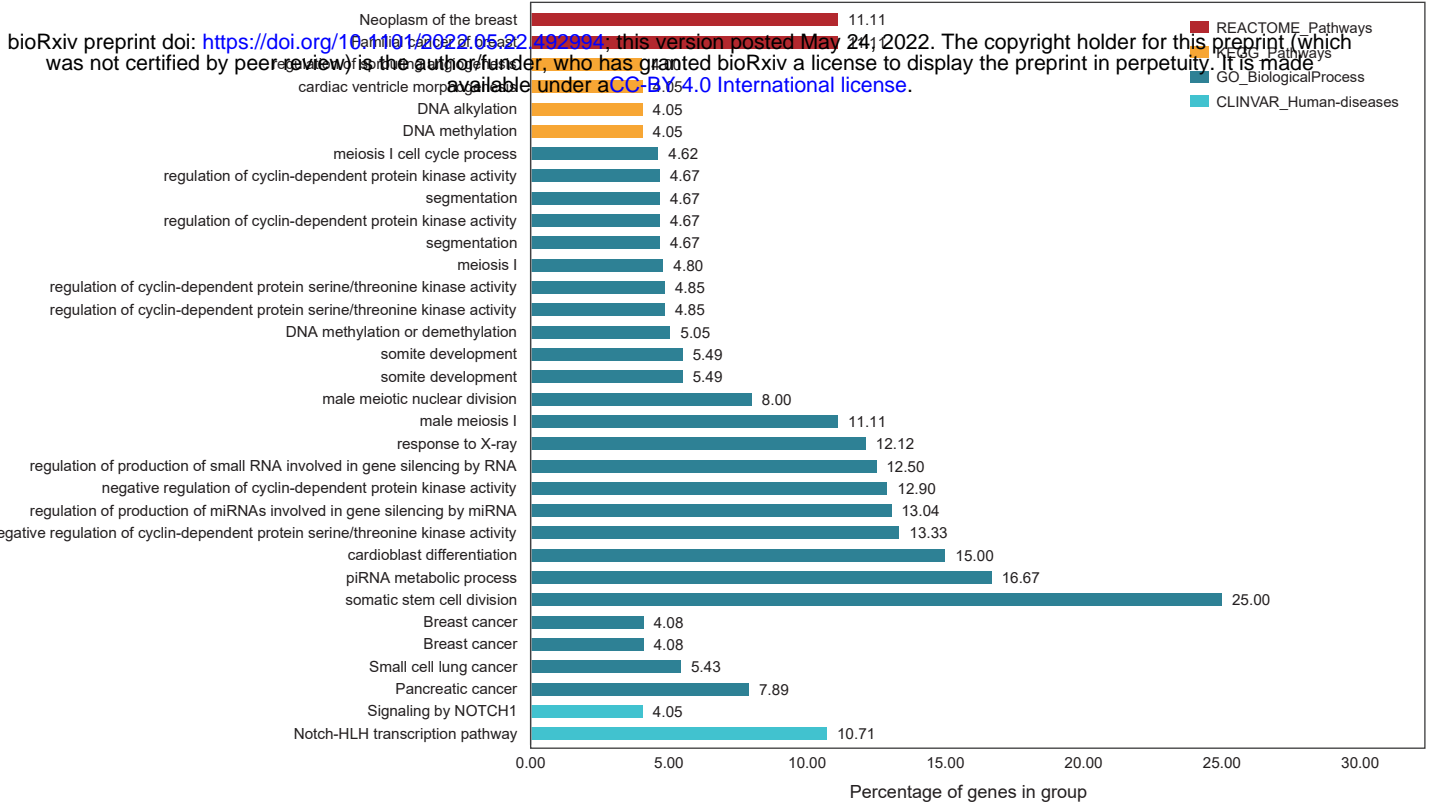


Figure 3. Optimal model feature weight analysis. The scatter points represent the SHAP value of each feature for each sample. Features are sorted according to the sum of the magnitudes of the SHAP values of all samples. The first 30 features are shown, and the colors represent the feature values (red high, blue low). For example, as age ("AGE_AT_DIAGNOSIS") increases, the risk of death within five years of the sample will increase.

A



B

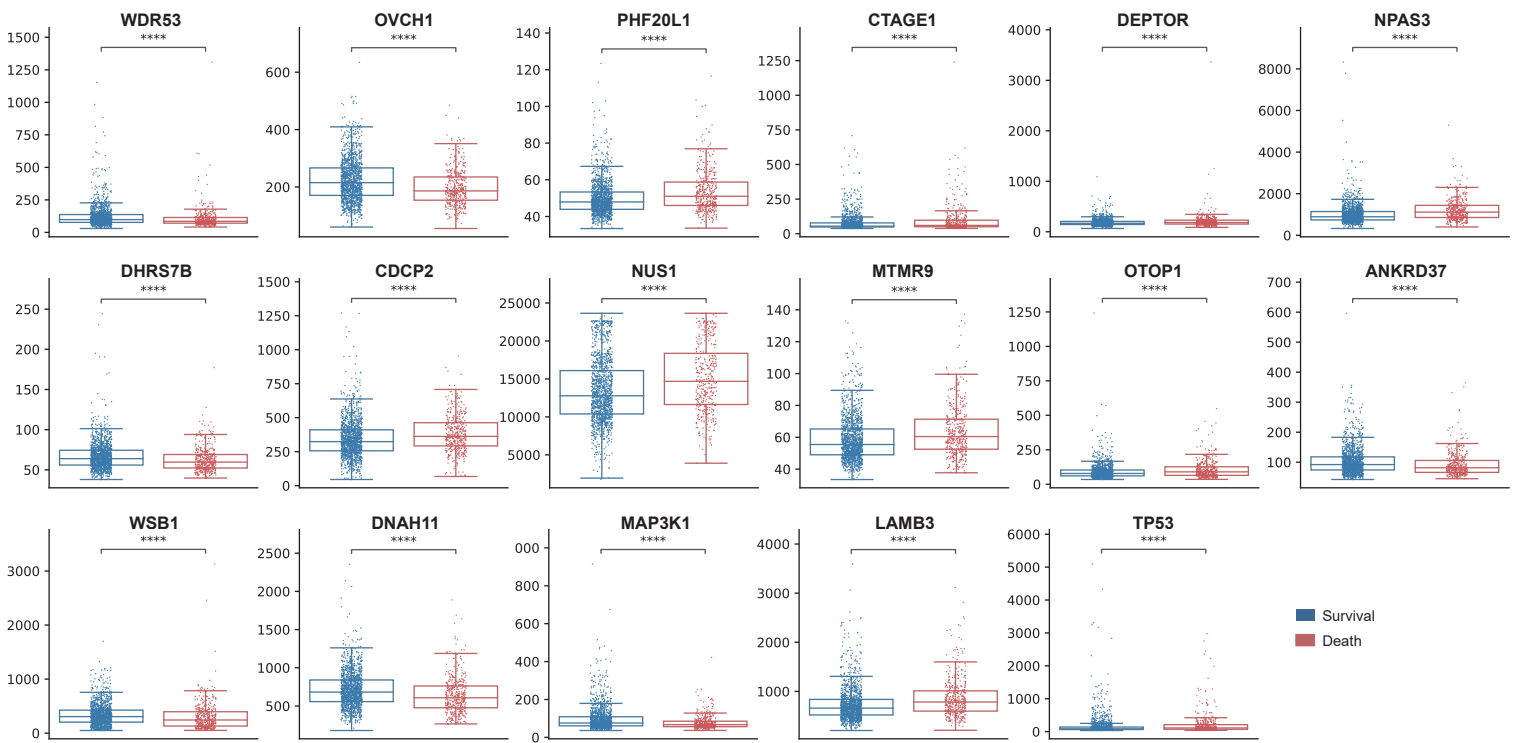


Figure 4. A) Optimal Model Pathway Enrichment Analysis; B) Transcriptome-level differential analysis of optimal model features.

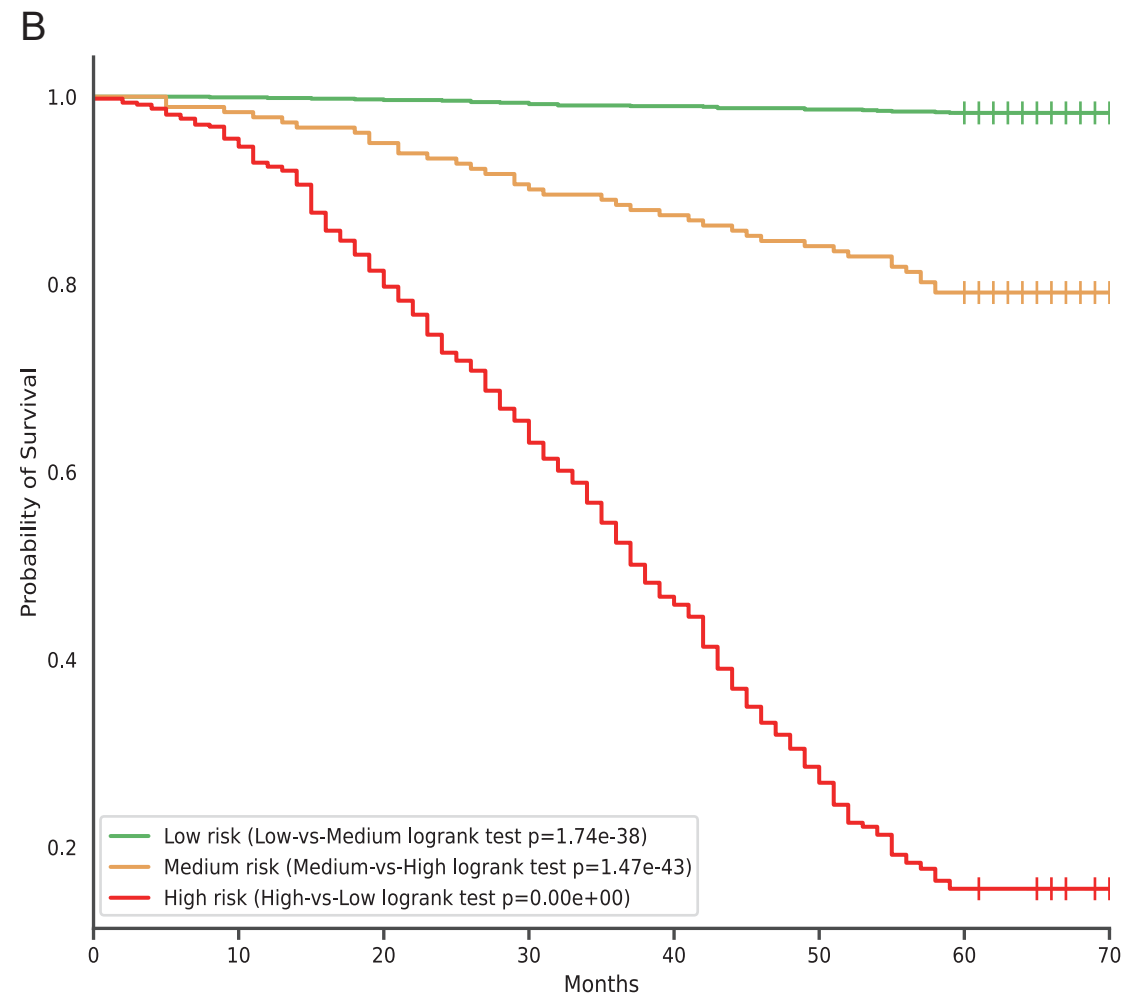
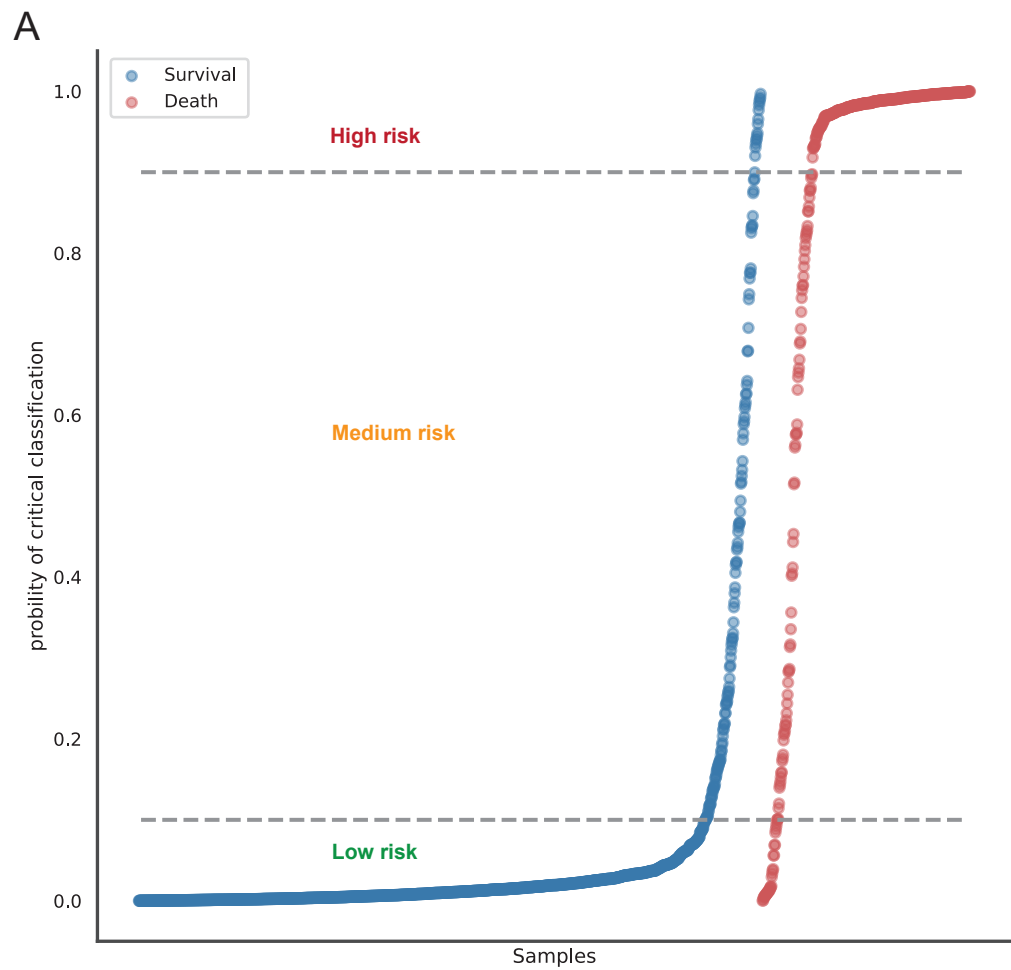


Figure 5. A) Risk stratification for all samples based on model scoring; B) Plot Kaplan-Meier survival curves for three groups of stratified outcomes (high, intermediate, and low risk).